IeCAT 2020

sciforum

*Conference Proceedings Paper*

# Linear motors based on piezoelectric MEMS

**Víctor Ruiz-Díez [1]*, Jorge Hernando-García [1] and José Luis Sánchez-Rojas [1]**

[1] Microsystems, Actuators and Sensors Group, Universidad de Castilla-La Mancha, E-13071 Ciudad Real, Spain; victor.ruiz@uclm.es (V.R.-D.); jorge.hernando@uclm.es (J.H.-G.); joseluis.saldavero@uclm.es (J.L.S.-R.)

* Correspondence: victor.ruiz@uclm.es; Tel.:+34-926-295-300

**Abstract:** This paper reports the design, fabrication and performance of MEMS-based piezoelectric bidirectional conveyors featuring 3D printed legs in bridge resonators. The structures consisted of aluminium-nitride (AlN) piezoelectric film on top of millimetre-sized rectangular thin silicon bridges and two electrode patches. The position and size of the patches were analytically optimised for the wave generation, while the addition of 3D-printed legs, for a controlled contact, allowed for a further step into the manufacturing of efficient linear motors. Such hybrid devices have recently demonstrated the conveyance of sliders – surpassing several times the motor weight – with speeds of 1.7 mm/s, while operated at 6 V and 19.3kHz. However, by the optimisation of various aspects of the device such as the vibrational modes and excitation signals speeds above 25 mm/s were demonstrated.

**Keywords:** travelling wave; standing wave; bidirectional linear motion; conveyor; piezoelectric; AlN; MEMS

## 1. Introduction

The miniaturization of actuators for applications that need large displacements, high energy efficiency or output forces is an ongoing challenge **[1]**. Piezoelectric ultrasonic motors (USM) have proven to be a suitable solution to obtain long motion range, high torque, quick response, high power to weight ratio and high efficiency in comparison to electrostatic, magnetic, and thermal alternatives **[2–4]**. Despite the advantages of USM for linear motion, scaling down to the millimetre range remains a challenge, due to the difficulties in generating standing or travelling waves at high frequencies with enough amplitude **[5].**

In pursuit of miniaturization, the monolithic fabrication based on silicon micromachining was successfully applied to the effective size reduction of such positional devices. Different actuation techniques have benefited from the MEMS technology, demonstrating locomotion or conveyance in the millimetre scale with speeds of a few millimetres per seconds and payloads below 50 mg **[6–8]**. However, to reach a step further into the miniaturisation of efficient motors, piezoelectric actuation becomes a promising alternative **[9,10]**.

In this work, we present a hybrid design for linear locomotion based on piezoelectric MEMS resonators with 3D-printed legs. The MEMS-based resonator consists of a conductive silicon bridge, actuated thanks to an integrated AlN piezoelectric film, sandwiched between the silicon film and the metallic electrodes. Analytical approaches were used to calculate the optimal electrode layout for the efficient generation of the mechanical waves, i.e. standing-wave or travelling-wave, in the motor. The movement of the surface of the silicon plate was transferred to a slider through an array of 3D-printed legs attached to its surface, allowing a controlled contact between stator and slider and the amplification of the elliptical or diagonal movement caused by the TW or the SW, respectively. The conveyance of light sliders was demonstrated, and the kinetic capabilities of the motor were characterised under both operation modes.

## 2. Device design

Here we focus on the linear motors based on piezoelectrically actuated bridges with a length $L = 10\ mm$ and a width $W = 2\ mm$. The structure consisted of a silicon substrate with a thickness $t_s = 30\ \mu m$, an aluminium-nitride (AlN) piezoelectric film with a thickness $t_p = 1\ \mu m$ and two 500 nm thick Gold (Au) electrode patches on top, that were neglected in the mechanical analysis. Figure 1a depicts the layout.

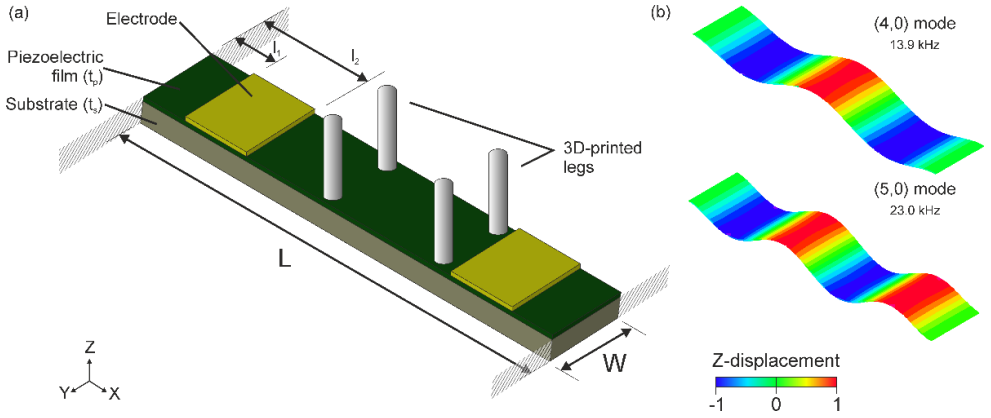


**Figure 1. (a)** Schematic diagram of the device design. A bridge structure of length L and width W consisting of a silicon substrate with a thickness $t_s$, covered by an AlN piezoelectric layer of thickness $t_p$. Two symmetrically disposed metallic electrodes were placed close to the edges, starting at a distance $l_1$ and ending at a distance $l_2$. 3D-printed resin legs were manually attached in a subsequent step. **(b)** Mode shapes involved in the motor design. Resonant frequencies are also included. Colour bar represents the normalised modal displacement in the Z-axis.

The generation of bidirectional linear motion would rely on the flexural vibration modes of the bridge structure in Figure 1a. In particular, the third and fourth-order bending modes, i.e. (4,0) and (5,0) modes using Leissa nomenclature [11]. Figure 1b shows the modal shapes and their respective resonant frequencies.

The actuation principle of the motor is based on the generation of mechanical waves – either standing-wave (SW) or travelling-wave (TW) types – on the piezoelectrically actuated structure, together with the inclusion of 3D-printed millimetre long legs. These legs will ensure the contact between the vibrating structure and the stator while transmitting a translational motion to the slider.

The generation of linear TW in beams by the combination of two flexural vibration modes was already reported, using two symmetrically placed piezoelectric patches [10]. Here we followed the same approach, obtaining the patch position and size that optimises the TW quality and amplitude with the targeted modes in Figure 1b. Regarding the leg position, those should be placed where the TW envelope is ideally constant, to ensure an elliptical trajectory at the tip [12]. That condition is met at the central plateau of the TW envelope, the area between the two patches [10].

Linear motion can also be obtained by inducing an SW in the resonator and choosing an appropriate distribution of legs [13]. A stiff leg placed between a node and a peak of the modal shape wave (Figure 1b) would describe a diagonal trajectory. Depending on the chosen side of the crest, the thrust exerted to the rotor would be in the positive or negative direction of the wavelength. Therefore, to achieve bidirectional motion, two different flexural modes can be used. By placing the legs at any of the intersecting regions between each mode chosen side crests, the same device could be used as an SW motor, with two different directions of movement depending on the vibration mode excited.

According to reference [10], the optimal patches for the TW generation could be suitable for the SW generation too. Besides, in order to maximize the excitation of the SW and taking advantage of the two-patch configuration, a phase optimisation was performed [14]. Finally, the combination of this patch design together with attached legs in the intersecting crests regions (SW operation mode) within the central plateau (TW operation mode), would allow the same motor to be operated under SW or TW conditions.

## 3. Materials and methods

Monolithic microfabrication techniques were used to implement rectangular microplates according to the geometry and materials previously described, clamped at both sides. For all the devices, the layer structure was as follows: a 30 μm thick, p-doped (100), silicon plate served as the bottom electrode, which was covered with a 1 μm thick AlN piezoelectric film. As the top electrode, a 500 nm thick Au electrodes were deposited. Dices with two different devices were glued and wire-bonded to a printed circuit board (PCB) to facilitate the electrical access (Figure 2).

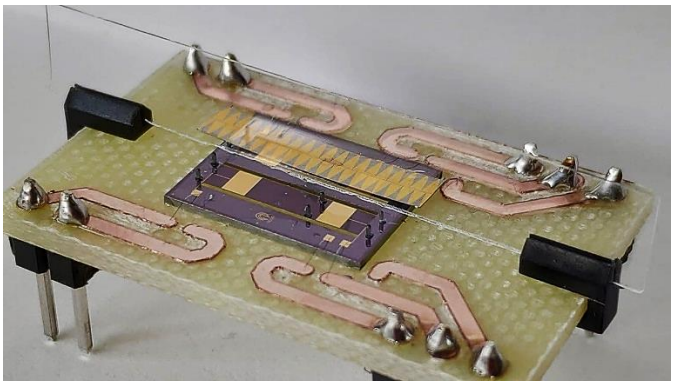

**Figure 2.** Photograph of the fabricated motor with attached legs. A silicon dice containing two designs was wire bonded to a PCB. In the experimental setup, a gold-patterned slider was placed on top of the motor and constrained to a lane by a vertical glass slice.

Cylindrical legs with a length of 750 μm and a diameter of 300 μm were designed and manufactured using a B9 Core 530 DLP 3D printer, using proprietary Black Resin. The active pair of legs was glued on the bridge surface using a cyanoacrylate-based adhesive (see Figure 2) and two additional pairs were placed at the device frame, serving as passive supports.

In the kinetic characterization, a Tektronix AFG 3000 series arbitrary waveform generator (AWG) was used to generate the required waveforms to be applied to each of the electrode patches. In the experimental setup, the PCB containing a pair of such devices (see Figure 2) was placed on a levelled platform – in order to avoid an uneven movement of the slider – under the microscope camera. The orthogonal movement of the sliders was restricted to a rectilinear lane with the help of glass pieces. The movement of the slider was optically recorded by a microscope camera and the videos were processed by a motion tracking algorithm programmed in Matlab, in order to obtain the slider positions versus time. The mean speed was computed afterwards.

**4. Results**

The application of the motor to transport objects in contact with the device surface was assessed in the two operation modes, with sliders consisting of silicon plates of 15x3x0.02 $mm^3$ with a mass of 2 mg. In the TW operation mode, the motor was actuated at 19.55 kHz with 90° for the forward direction and -90° for the reverse direction. In the SW operation mode, the motor was actuated in the (4,0) mode at 15.25 kHz and no phase difference between patches for the reverse direction, and in the (5,0) mode at 24 kHz and a phase difference of 180° for the forward direction.

Figure 3 shows the results from the kinetic characterization in the forward direction (similar results were obtained in the reverse direction). As it can be seen, in the TW operation mode, the motor was able to develop conveyor speeds of 1.2 mm/s at 10V, while in the SW operation mode, the speed reached a maximum value of 27 mm/s. This speed of almost 3 BL/s (body-lengths per second) supposes a huge improvement, comparing to the TW operation mode, mainly due to the actuation of the motor in resonance.

Besides, the minimum excitation to generate locomotion of the slider was as low as 2V in the SW operation mode, with a linear dependence of the speed with the applied voltage up to 4V, when a speed of 20 mm/s was reached. From them, a decrease in the growth rate of the speed with voltage was found, what can be attributed to the low inertia of the light slider used in the tests.

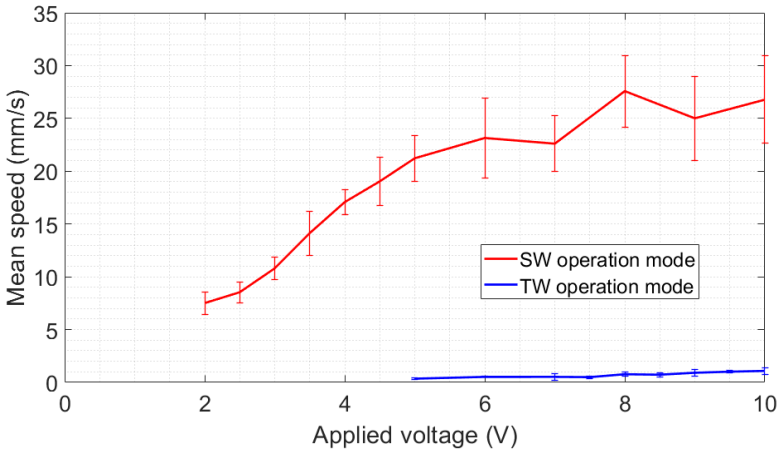


**Figure 3.** Results from the kinetic characterization of the motor with TW operation mode at 19.55 kHz with a phase difference of 90° and SW operation mode with the (5,0) mode at 24 kHz and a phase difference of 180°.

## 5. Conclusions

This work reports the design, fabrication and electrical and optical characterization of piezoelectric MEMS plates for linear motion applications. Successful generation of bidirectional TW was demonstrated on a monolithic microfabricated silicon-based bridge, combined with 3D printed legs, to overcome the intrinsic limitation of the suspended bridge to attain an efficient contact with objects. The bridge devices were also excited in resonance, inducing SW based on the third and fourth flexural modes. The 3D printed legs were placed at those positions in what the resonator could act as a bidirectional resonant motor.

The kinetic performance of the fabricated motor was studied with a 2 mg slider. The conveyor demonstrated bidirectional speeds of 1.2 mm/s when a TW was induced in the resonator at 10V and a frequency of 19.55 kHz. The same device could be operated in resonance, by inducing SWs based on the (4,0) and (5,0) modes at 15.25 and 24 kHz. In this operation mode, the conveyor demonstrated speeds as high as 27 mm/s for continuous sinusoidal excitation.

**Author Contributions:** Conceptualization, J.L.S.-R.; software, V.R.-D.; investigation, V.R-D.; writing—original draft preparation, V.R.-D.; writing—review and editing, J.L.S-R., J.H.-G., H.S. and A.A.; supervision, J.L.S.-R. and J.H.-G.; project administration, J.L.S.-R. and J.H.-G.; funding acquisition, J.L.S.-R. and J.H.-G. All authors have read and agreed to the published version of the manuscript.

**Acknowledgements:** This work was supported by the European Regional Development Fund, the Spanish Ministerio de Ciencia, Innovación y Tecnología project (RTI2018-094960-B-100), and the regional government (JCCLM) project (SBPLY/17/180501/000139).

**Conflicts of Interest:** The authors declare no conflict of interest.

## References

1. Kenji Uchino *MicroMechatronics, Second Edition*;
2. Chan, M.L.; Yoxall, B.; Park, H.; Kang, Z.; Izyumin, I.; Chou, J.; Megens, M.M.; Wu, M.C.; Boser, B.E.; Horsley, D.A. Design and characterization of MEMS micromotor supported on low friction liquid bearing. *Sens. Actuators Phys.* **2012**, *177*, 1–9, doi:10.1016/j.sna.2011.08.003.
3. Khiat, A.; Spronck, J.W.; van Schieveen, J.; Milosavljevic, S.; Wei, J.; Estevez, P.; Sarro, P.M.; Staufer, U. Linear and rotational thermal micro-stepper motors. *Microelectron. Eng.* **2012**, *98*, 497–501, doi:10.1016/j.mee.2012.07.086.
4. Sarajlic, E.; Yamahata, C.; Cordero, M.; Fujita, H. Three-Phase Electrostatic Rotary Stepper Micromotor With a Flexural Pivot Bearing. *J. Microelectromechanical Syst.* **2010**, *19*, 338–349, doi:10.1109/JMEMS.2010.2040139.

5. Pulskamp, J.S.; Polcawich, R.G.; Rudy, R.Q.; Bedair, S.S.; Proie, R.M.; Ivanov, T.; Smith, G.L. Piezoelectric PZT MEMS technologies for small-scale robotics and RF applications. *MRS Bull.* **2012**, *37*, 1062–1070, doi:10.1557/mrs.2012.269.
6. Kladitis, P.E.; Bright, V.M. Prototype microrobots for micro-positioning and micro-unmanned vehicles. *Sens. Actuators Phys.* **2000**, *80*, 132–137, doi:10.1016/S0924-4247(99)00258-7.
7. Ebefors, T.; Mattsson, J.U.; Kälvesten, E.; Stemme, G. A walking silicon micro-robot. In Proceedings of the in Proceedings of the 10th International Conference on Solid-State Sensors and Actuators (Transducers'99; 1999; pp. 1202–1205.
8. Yahiaoui, R.; Zeggari, R.; Malapert, J.; Manceau, J.-F. A MEMS-based pneumatic micro-conveyor for planar micromanipulation. *Mechatronics* **2012**, *22*, 515–521, doi:10.1016/j.mechatronics.2011.04.005.
9. Smith, G.L.; Rudy, R.Q.; Polcawich, R.G.; DeVoe, D.L. Integrated thin-film piezoelectric traveling wave ultrasonic motors. *Sens. Actuators Phys.* **2012**, *188*, 305–311, doi:10.1016/j.sna.2011.12.029.
10. Ruiz-Díez, V.; Hernando-García, J.; Toledo, J.; Ababneh, A.; Seidel, H.; Sánchez-Rojas, J.L. Bidirectional Linear Motion by Travelling Waves on Legged Piezoelectric Microfabricated Plates. *Micromachines* **2020**, *11*, 517, doi:10.3390/mi11050517.
11. Leissa, A.W.; Qatu, M.S. *Vibration of Continuous Systems*; McGraw Hill Professional, 2011; ISBN 9780071714808.
12. Hernando-García, J.; García-Caraballo, J.L.; Ruiz-Díez, V.; Sánchez-Rojas, J.L. Motion of a Legged Bidirectional Miniature Piezoelectric Robot Based on Traveling Wave Generation. *Micromachines* **2020**, *11*, 321, doi:10.3390/mi11030321.
13. Siyuan He; Weishan Chen; Xie Tao; Zaili Chen Standing wave bi-directional linearly moving ultrasonic motor. *IEEE Trans. Ultrason. Ferroelectr. Freq. Control* **1998**, *45*, 1133–1139, doi:10.1109/58.726435.
14. Ruiz-Díez, V.; Manzaneque, T.; Hernando-García, J.; Ababneh, A.; Kucera, M.; Schmid, U.; Seidel, H.; Sánchez-Rojas, J.L. Design and characterization of AlN-based in-plane microplate resonators. *J. Micromechanics Microengineering* **2013**, *23*, 074003, doi:10.1088/0960-1317/23/7/074003.